AGU PUBLICATIONS

JGR

Journal of Geophysical Research: Space Physics

RESEARCH ARTICLE
10.1002/2013JA019731

Key Points:
- Statistical study of properties of the VLF QP emissions
- The largest collection of satellite observations of QP emissions
- QP events with larger modulation periods have lower frequency drifts

Correspondence to:
M. Hayosh,
hayosh@ufa.cas.cz

Citation:
Hayosh, M., F. Němec, O. Santolík, and M. Parrot (2014), Statistical investigation of VLF quasiperiodic emissions measured by the DEMETER spacecraft, *J. Geophys. Res. Space Physics*, *119*, 8063–8072, doi:10.1002/2013JA019731.

Received 23 DEC 2013
Accepted 27 AUG 2014
Accepted article online 1 SEP 2014
Published online 6 OCT 2014

Statistical investigation of VLF quasiperiodic emissions measured by the DEMETER spacecraft

M. Hayosh[1], F. Němec[2], O. Santolík[1,2], and M. Parrot[3]

[1]Institute of Atmospheric Physics, Academy of Sciences of the Czech Republic, Prague, Czech Republic, [2]Faculty of Mathematics and Physics, Charles University in Prague, Prague, Czech Republic, [3]LPC2E/CNRS, Orléans, France

Abstract We present a survey of quasiperiodic (QP) ELF/VLF emissions detected onboard the DEMETER (Detection of Electro-Magnetic Emissions Transmitted from Earthquake Regions) satellite (altitude of about 700 km, nearly Sun-synchronous orbit at 10:30/22:30 LT). Six years of data have been visually inspected for the presence of QP emissions with modulation periods higher than 10 s and with frequency bandwidths higher than 200 Hz. It is found that these QP events occur in about 5% of daytime half orbits, while they are basically absent during the night. The events occur predominantly during quiet geomagnetic conditions following the periods of enhanced geomagnetic activity. Their occurrence and properties are systematically analyzed. QP emissions occur most often at frequencies from about 750 Hz to 2 kHz, but they may be observed at frequencies as low as 500 Hz and as high as 8 kHz. Modulation periods of QP events may range from about 10 to 100 s, with typical values of 20 s. Frequency drifts of the identified events are generally positive, but they are lower for events with larger modulation periods. The events are usually limited to higher L values ($L > 2$). The upper L shell boundary of their occurrence could not be identified using the DEMETER data, but they are found to extend up to at least $L \sim 6$. The occurrence rate of the events is significantly lower at the longitudes of the South Atlantic anomaly (by a factor of more than 2).

1. Introduction

Quasiperiodic (QP) emissions are ELF/VLF electromagnetic waves at frequencies of about 500 Hz–4 kHz generated in the outer magnetosphere, which exhibit a periodic time modulation of the wave intensity [*Helliwell*, 1965; *Carson et al*., 1965; *Sazhin and Hayakawa*, 1994; *Smith et al*., 1998; *Sato et al*., 1974]. The modulation period of the QP emissions varies in the range of about 10–80 s, and they are observed at L shells > 3 [*Ho*, 1973; *Kimura*, 1974; *Morrison et al*., 1994; *Engebretson et al*., 2004]. This modulation period corresponds approximately to the Pc3–Pc5 oscillations geomagnetic pulsations [*Morrison*, 1990; *Manninen et al*., 1994]. QP emissions which appear to be closely associated with coincident ULF geomagnetic pulsations are called "QP type one" (QP1), whereas QP emissions which are not accompanied by geomagnetic pulsations are called "QP type two" (QP2) [*Kitamura et al*., 1969; *Sato et al*., 1974]. The source region of both QP1 and QP2 emissions is probably located close to the geomagnetic equatorial plane [*Sato and Kokubun*, 1980; *Sato and Fukunishi*, 1981]. QP1 emissions usually occur during magnetically disturbed conditions ($Kp \approx 2$–4), while QP2 emissions are observed mostly during geomagnetically quiet periods ($Kp \leq 2$) [*Manninen et al*., 2012]. QP1 emissions are likely to originate due to quasiperiodic fluctuations of resonant conditions of wave growth in the wave generation region [*Kimura*, 1974; *Chen*, 1974; *Sato and Fukunishi*, 1981; *Sazhin*, 1987; *Watt et al*., 2011]. The emissions of this type are often observed simultaneously in geomagnetically conjugated regions [*Sato and Kokubun*, 1981]. The generation mechanism of the QP2 emissions is still not entirely understood. Synchronous variations of VLF wave amplitudes, magnetic field magnitude, and precipitating energetic electron fluxes are likely to play a role in their generation. In particular, *Bespalov and Trakhtengerts* [1976], *Davidson* [1979], and *Demekhov and Trakhtengerts* [1994] developed a self-consistent model to explain the QP modulation of the wave intensity and electron precipitation by the periodic wave generation in the regime of relaxation oscillations. *Bespalov* [1982] proposed a model of QP2 emissions excitation by periodic self-sustained cyclotron instability (due to the modulation of the distribution function anisotropy). Constant shapes for the wave spectrum and energetic particle distribution were used in the model. *Hayosh et al*. [2013] reported simultaneous observations of QP emissions and modulated fluxes of the energetic electrons coming from the region with favorable conditions for the development of the cyclotron instability. This result is in agreement with theoretical

work by *Pasmanik et al*. [2004]. *Sato and Matsudo* [1986] described a QP event associated with quasiperiodic electron precipitation induced by a VLF wave-electron interaction near the equatorial plane in the magnetosphere. They supposed that the electron precipitation produces the ULF magnetic variations observed on the ground. However, the generation mechanisms of QP1 and QP2 are still neither clearly separated nor understood. For instance, *Tixier and Cornilleau-Wehrlin* [1986] analyzed both satellite and ground-based data and demonstrated that the classification between QP1 and QP2 is not so obvious in space, suggesting that both types of emissions might have the same generation mechanism.

In order to better understand the properties of QP emissions, it is important to separate their spatial and temporal variations. Ground-based observations using longitudinally spaced stations can be a very effective tool to study temporal properties of QP emissions [i.e., *Smith et al*., 1991; *Manninen et al*., 2013, 2014]. Concerning the satellite measurements, spatiotemporal variations of QP emissions can be distinguished by using simultaneous measurements of the same event by several different spacecraft. *Němec et al*. [2013a] have analyzed a large-scale long-lasting QP event observed simultaneously by the DEMETER (Detection of Electro-Magnetic Emissions Transmitted from Earthquake Regions) and the Cluster spacecraft, showing that the same QP modulation of the wave intensity is observed at the same time at very different locations in the inner magnetosphere. *Němec et al*. [2013b] performed a survey of QP events identified by the Cluster Wide Band Data (WBD) instrument, demonstrating that at least a part of them propagates unducted. In only 4 out of the 21 analyzed events, they have identified ULF magnetic field pulsations with frequencies roughly corresponding to the modulation period of the observed QP events. These results show that QP emissions can be long lasting and fill large volumes of the magnetosphere. Hence, they can influence magnetospheric particles and cause their precipitation.

Previous satellite measurements allowed us to determine the wave mode of the analyzed QP events. Inside the low-latitude region of the inner magnetosphere at $L \sim 4$ the waves propagate in the right-hand polarized whistler mode above the local lower hybrid frequency [*Němec et al*., 2013a]. At a low-altitude spacecraft the QP emissions are also seen [*Pasmanik et al*., 2004; *Hayosh et al*., 2013] in the right-hand polarized mode, propagating at high latitudes as Type A emissions of *Santolík and Parrot* [1999, 2000] from the inner magnetosphere [*Santolík et al*., 2006b] .

Satellite measurements allow us to sample a large range of latitudes. They can be used to estimate the size of a region where the QP emissions occur and, moreover, to collect data at magnetically conjugated points. We present a systematic survey of QP emissions based on more than 6 years of data from the low-altitude DEMETER spacecraft. According to our knowledge, this represents the largest satellite database of QP events collected up to now.

2. Data Set

DEMETER was a low-altitude French satellite launched by Centre National des Etudes Spatiales in June 2004 on a nearly Sun-synchronous circular orbit (10:30 and 22:30 LT). The initial altitude of the spacecraft (710 km) was decreased to 660 km in December 2005 [*Parrot*, 2006]. The mission came to the end in December 2010, i.e., about 6.5 years of measured data are available.

The satellite operated in two different modes, called Burst and Survey. Although higher-resolution data were measured during the Burst mode, it could not be effectively used for the intended systematic study due to the limited spatial coverage. The Survey mode data have been therefore used. The Survey mode was active all the time at geomagnetic latitudes lower than 65°. In the frequency range of interest, the power spectrum of one electric and one magnetic field component with a predefined frequency resolution (19.53 Hz) was calculated on board every 0.5 s or 2 s, depending on the mode of the instrument [*Parrot et al*., 2006; *Berthelier et al*., 2006]. Since the magnetic field data generally contain a significant amount of interferences between 1.7 and 8 kHz, the sensitivity of electric field data is found to be much better, and exclusively, the electric field data will be used in the presented study.

All the Survey mode electric field data measured during the whole DEMETER mission have been visually inspected for the presence of QP emissions. We have used a fixed range of power spectral densities between 0.0023 and 0.234 $\mu V^2\ m^{-2}\ Hz^{-1}$ for this selection. Therefore, QP emissions with intensities lower than the lower threshold value have not been detected. As a single DEMETER half orbit sometimes contains two QP events, located approximately in geomagnetically conjugated regions, the total number of identified QP events is larger than the number of QP half orbits. Altogether, there were 2181 daytime QP events out of

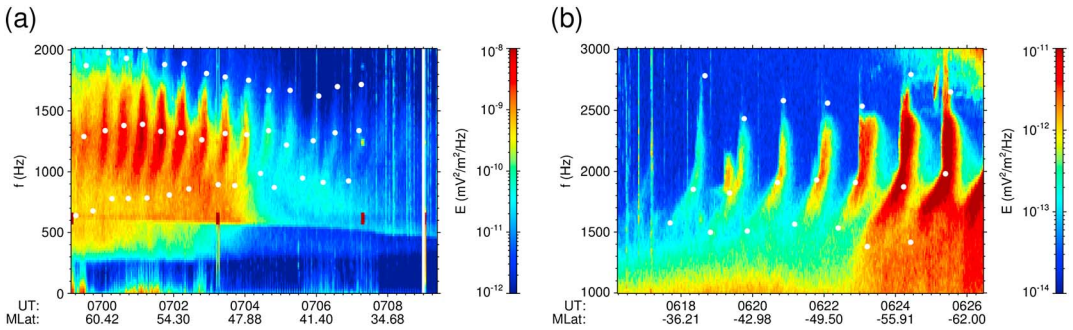

Figure 1. Two examples of detailed frequency-time spectrograms corresponding to QP events. (a) The data were measured on 1 September 2004 between 06:59:00 UT and 07:09:10 UT in the Northern Hemisphere. A set of individual QP elements can be seen at frequencies between about 700 Hz and ~2000 Hz, starting at the beginning of the plotted time interval and slowly fading out toward lower geomagnetic latitudes. (b) The data were measured on 13 April 2006 between 06:16:15 UT and 06:26:30 UT in the Southern Hemisphere. QP elements can be seen at frequencies between about 1500 Hz and 3000 Hz. Similar to Figure 1a they slowly fade toward lower geomagnetic latitudes (at the beginning of the time interval).

29,001 daytime half orbits and 83 nighttime QP events out of 28706 nighttime half orbits. This means that about 40% of the half orbits contained QP emissions both in the Northern and Southern Hemispheres. Moreover, only 772 half orbits with QP emissions were "isolated"; i.e., there were no QP emissions observed in the surrounding orbits. This clearly indicates a significant extent and duration of the emissions.

Note that due to the fact that the QP events were identified visually in overall frequency-time spectrograms corresponding to whole half orbits, we were likely to miss QP events with modulation periods lower than about 10 s or those with the frequency bandwidths lower than about 200 Hz. For the purpose of the present paper, QP event is defined as a continuous phenomenon spanning from the first observed QP element to the last observed QP element, with gaps significantly larger than the modulation period both before and after the event. Having visually identified QP events in the whole DEMETER data set, detailed frequency-time spectrograms for the corresponding time intervals have been prepared. These have been used to manually (by using a mouse pointer on a computer screen) and individually mark all QP elements forming the events. Each QP element has been characterized by three frequency-time points. The first and the last points correspond to the beginning (lowest frequency) and ending (highest frequency) point of a QP element, respectively. These frequencies are defined as the minimum and the maximum frequencies still exhibiting a distinguishable QP modulation. A rough estimate of experimental uncertainties is three frequency bins of the spectrogram (~60 Hz). The middle point is used to characterize a change of the frequency sweep rate of an element, which is sometimes observed. The time of each point is determined by the time of the maximum intensity at a given frequency with an accuracy of the spectrogram resolution (2 s). All the statistical results presented in this paper are based on these three-point characterizations of the QP elements. We are unable to distinguish between the QP1 and QP2 cases in our database because the ULF pulsations of the ambient magnetic field cannot be measured by the DEMETER spacecraft. Additionally, the ground-based measurements are only available for a very limited subset of our database, and their analysis is out of scope of this paper.

Two examples of detailed frequency-time spectrograms corresponding to QP events are shown in Figure 1. The QP event shown in Figure 1a was observed in the Northern hemisphere on 1 September 2004 between 06:59 UT and 07:08 UT. A set of nearly vertical QP elements with a modulation period of about 23 s can be seen, starting at the beginning of the plotted time interval and slowly fading out toward lower geomagnetic latitudes in the end of the presented time interval. The QP event shown in Figure 1b was observed in the Southern Hemisphere on 13 April 2006 between 06:17:00 UT and 06:26:30 UT. Again, a set of nearly vertical QP elements can be seen, slowly increasing their intensity from lower geomagnetic latitudes (Figure 1a). The modulation period of this QP event is about 35 s. The white points overplotted in both figures correspond to the results of the manual identification of QP elements.

3. Results

This database enabled us to analyze occurrence and properties of QP emissions. First, we have verified whether the geomagnetic conditions during the occurrence of the QP events differ from the normal ones.

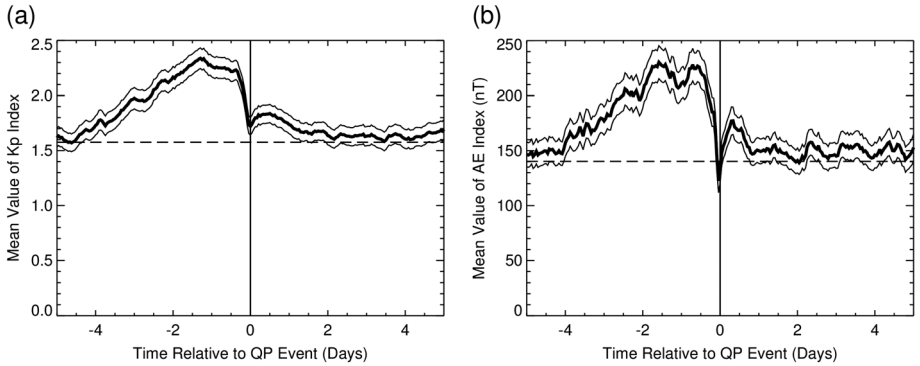

Figure 2. (a) Mean value of the *Kp* index as a function of the time relative to the QP events is shown by the bold line. The corresponding $\pm 3\sigma$ interval is marked by the thin lines. (b) The same as Figure 2a, but for the *AE* index.

A superposed epoch analysis was used to check the dependence of the mean values of the *Kp* and *AE* indexes on the time relative to the times of the QP events. Results calculated using 1 h time bins spanning from 5 days before to 5 days after the times of the QP events are shown in Figure 2. The dependence obtained for the mean value of the *Kp* index is plotted in Figure 2a by a bold line, the dependence obtained for the mean value of the *AE* index is plotted by a bold line in Figure 2b. Thin lines plotted in both figures correspond to the interval of $\pm 3\sigma$ around the mean. This interval calculated from the standard deviation of the corresponding set of values divided by the square root of the number of the QP events in a given bin. Although the resulting $\pm 3\sigma$ intervals are rather small, this is principally due to the large number of QP events included in the study: usual variations of *Kp*/*AE* values are significantly larger. It can be seen that the geomagnetic activity before a QP event is on average slightly increased, and it returns back to its long-term average level (horizontal dashed line) very shortly before a QP event. Although this effect is statistically significant, one should keep in mind that its amplitude is very low compared to usual variations of *Kp*/*AE* index values, and it is again observable only owing to a large number of QP events included. Finally, we note that a similar result is obtained also for the *Dst* index (not shown).

The observed frequencies of QP elements are shown in Figure 3a. For a predefined frequency *f*, QP elements with *f* between their minimum and maximum frequencies have been counted. This number has been normalized by the total number of QP elements. Figure 3a shows this ratio as a function of *f*. It can be seen that most of the elements occurred at frequencies between about 600 and 3000 Hz with relative occurrence ratios more than 10%. Frequencies slightly above 1 kHz occur in most of the 75% of cases. Histograms of minimum and maximum frequencies of QP elements are shown in Figure 3b by a blue line and red line, respectively. The histogram of minimum frequencies of QP elements is rather sharply peaked with a clear maximum near 600 Hz. The histogram of maximum frequencies shows a broad peak between 1.2 and 2 kHz.

A histogram of frequency bandwidths of QP events is shown in Figure 4a. It can be seen that the bandwidth of QP events most often is between several hundreds of Hertz and 1 kHz, but it can be as large as nearly 4 kHz

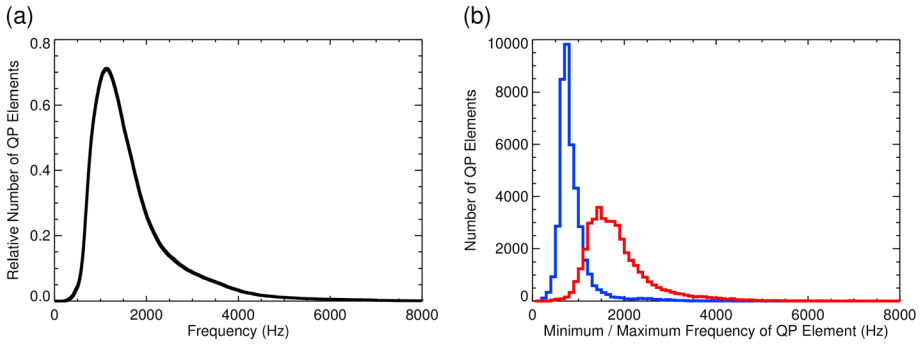

Figure 3. (a) Frequencies of observed QP elements (see text). (b) Median of minimum (blue) and maximum (red) frequencies of QP elements.

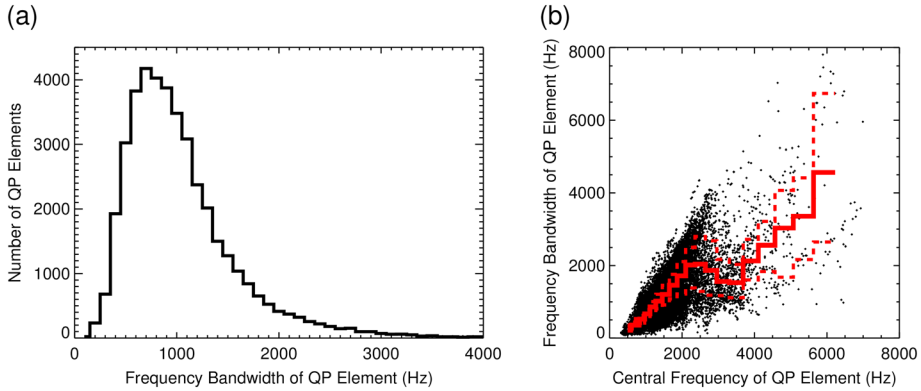

Figure 4. (a) Histogram of frequency bandwidths of QP elements. (b) Frequency bandwidth of QP elements as a function of their central frequencies. The red curve corresponds to a median dependence. Dashed red curves show the lower (0.25) and upper (0.75) quartiles.

in exceptional cases. We would like to note that we are missing QP events with frequency bandwidths lower than about 200 Hz during the identification. This is a likely reason for the rapid decrease of the number of observed events with very low bandwidths. The relationship between the frequency bandwidth of QP elements and their central frequency (i.e., the arithmetic average of the minimum and the maximum frequencies) is presented in Figure 4b. The red line corresponds to the median values calculated in consecutive frequency intervals. The frequency width of the first bin is 100 Hz, and the frequency width of each following interval is increased by 10% in order to account for a lower number of QP elements at high frequencies. It is found that the frequency bandwidth is larger for QP events with larger central frequencies. For central frequencies above 4 kHz the number of data points decreases rapidly, and the width of their distribution becomes larger.

A histogram of modulation periods of QP events is shown in Figure 5a. These have been determined for each of the events as a median of time separations between consecutive QP elements. It is found that the modulation periods range between about 10 and 100 s, with modulation periods of about 20 s occurring most often. However, it should be noted that the time modulation of a QP event may slightly vary over the time duration of an event. This is investigated in Figure 5b, which shows a histogram of the difference between 0.75 quartile of the modulation period and 0.25 quartile of the modulation period normalized by the median modulation period. This ratio estimates value of possible change of the QP emission modulation period during a QP event. It can be seen that a typical variation of the modulation period within a QP event is around 20%. The reason of this variation can be spatial as well temporal effects, but based only on DEMETER data we are not able to make any clear conclusion.

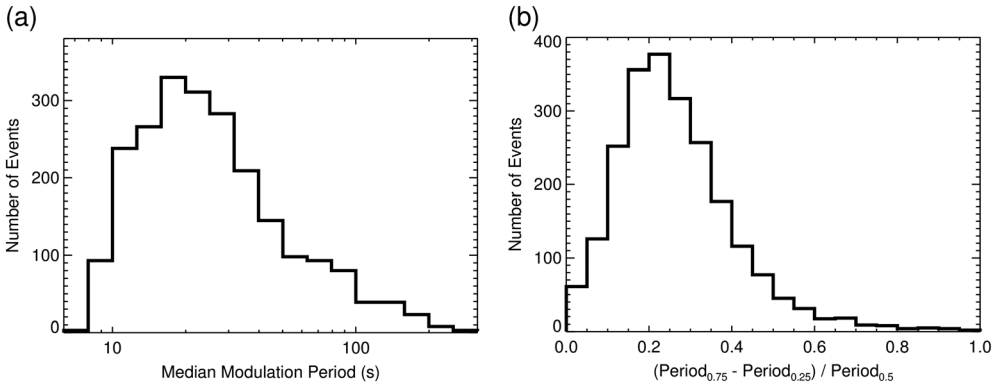

Figure 5. (a) Histogram of QP modulation periods (see text). (b) Histogram of typical variations of modulation period within a QP event normalized by the median value (see text).

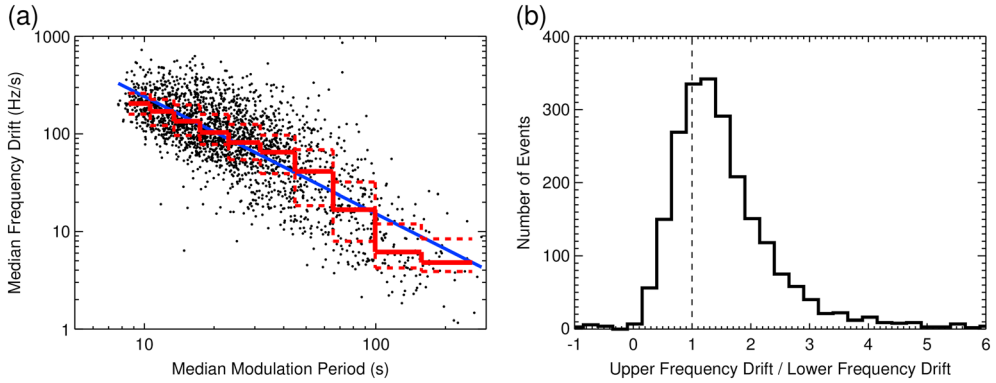

Figure 6. (a) Frequency drifts of QP events as a function of their modulation periods. The red line corresponds to median values calculated in consecutive intervals of modulation period. Dashed red curves show the lower (0.25) and upper (0.75) quartiles. The blue line shows a power law fit of the frequency drift as a function of median period (the value of the exponent resulting from the fit is about −1.2). (b) Histograms of the ratio between upper and lower values of the frequency drifts of QP emissions. Black dashed line corresponds to the value of this ratio equal to 1.

The relationship between median frequency drifts and median modulation periods of QP events is presented in Figure 6a. The calculated frequency drifts are always positive. Most of them occur in the interval between about 30 and 300 Hz·s^{-1}, with the frequency drifts of about 100 Hz/s occurring most often. Dashed red curves show the lower (0.25) and upper (0.75) quartiles. Since the number of detected QP events with large modulation periods is rather low, the size of the bins used to calculate the median and quartile values was chosen to exponentially increase, which ensures a reasonable number of data points in all bins. It is found that the events with larger modulation periods generally have lower frequency drifts. The corresponding power law fit with a coefficient of about −1.2 is plotted by a blue curve.

A histogram of frequency drifts of upper parts of QP events normalized by the frequency drifts of lower parts of QP events is shown by a red line in Figure 6b. The appropriate drift values are calculated as median frequency drifts of upper/lower parts of individual QP elements forming a given event. It is found that the upper parts have typically larger frequency drifts than the lower parts.

The dependence of the median power spectral density of individual QP elements on the median modulation periods of appropriate QP events is shown in Figure 7a. The dependence of the median power spectral density of individual QP elements on their frequency bandwidth is shown in Figure 7b. The overplotted solid red lines correspond to median values. The overplotted red dashed lines show 0.25 and 0.75 quartiles.

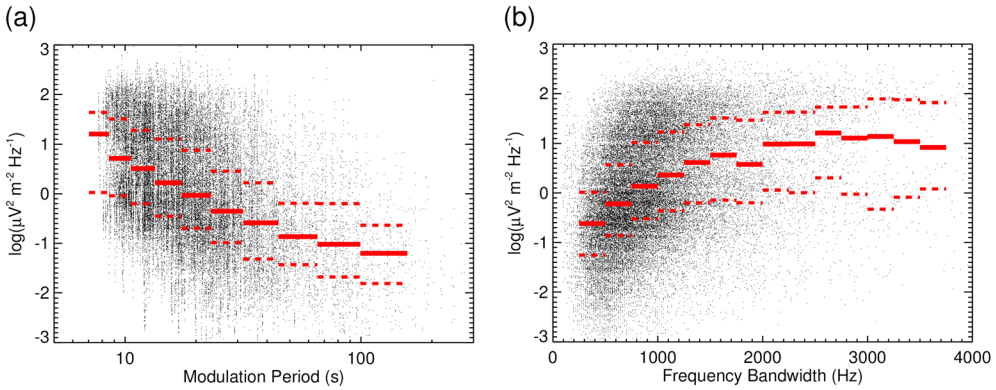

Figure 7. (a) Median power spectral density of electric field fluctuations of individual QP elements as a function of the median modulation periods of appropriate QP events. (b) Median power spectral density of electric field fluctuations of individual QP elements as a function of their frequency bandwidths. The solid red lines correspond to median values. The dashed red lines correspond to 0.25 and 0.75 quartiles.

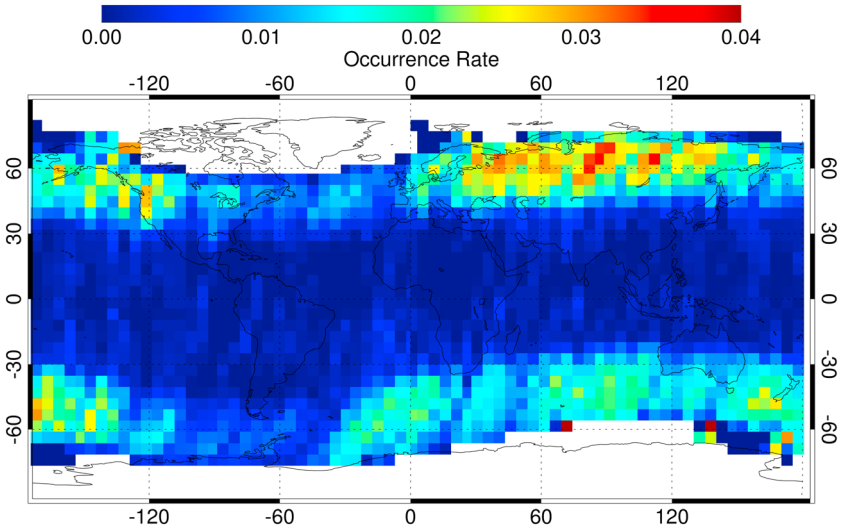

Figure 8. Geographical map of the location of QP events (the occurrence rate is color coded according to the scale above). The white areas at large latitudes are due to the fact that DEMETER did not measure at geomagnetic latitudes larger than about 65°.

It is found that the QP events with larger modulation periods generally have lower intensities. In agreement with the results from Figure 6a, this implies that there is also a strong correlation between the median intensity of QP elements and their frequency drift, with higher frequency drift elements being more intense (not shown).

The median power spectral density of individual QP elements increases with their frequency bandwidth up to the frequency bandwidth of about 2 kHz, and it remains nearly constant at larger frequency bandwidths. The elements with lower median intensities ($<1\ \mu V^2\ m^{-2}\ Hz^{-1}$) typically have frequency bandwidths less than about 1 kHz, whereas the elements with higher median intensities ($>1\ \mu V^2\ m^{-2}\ Hz^{-1}$) are observed in the whole range of frequency bandwidths.

A geographical distribution of the occurrence rate of QP emissions is shown in Figure 8. It is seen that QP emissions are observed mostly at geomagnetic latitudes larger than 30°. However, a small number of QP emissions is observed also at lower geomagnetic latitudes, and even at the geomagnetic equator. The absence of the QP emissions at large geomagnetic latitudes is due to the fact that the DEMETER measurements were limited to geomagnetic latitudes lower than about 65°. Concerning the longitudinal dependence of the occurrence rate, there seems to be a lower number of events observed at the longitudes of the Atlantic Ocean.

Most of the QP events are observed at *L* values between about 1.8 and 4. Although the number of QP events identified at larger L shells is rather low, there is a simultaneous decrease of the total number of DEMETER measurements. The resulting occurrence rate depicted in Figure 9b therefore remains nearly constant up to *L* shells of about 6. At *L* values larger than 6 the occurrence rate starts to decrease systematically. However, it should be noted that the total number of DEMETER measurements at those high *L* values is extremely limited. Moreover, one should emphasize that as QP events are composed of individual QP elements, which are separated in time, the identified beginning and ending times are necessarily biased by as much as the modulation period. Consequently, the identified spatial extent of a QP event is somewhat smaller than its real spatial extent, which will especially at high *L* values result in a slight underestimation of the occurrence rate of QP events.

The identified, only on the dayside, QP events as a function of *L* shell are shown by the black line in Figure 9a. Since the electric field measurements were not performed at all *L* values uniformly, and the data were obtained at high *L* values only during some of the orbits, the relative number of DEMETER passes where the electric field measurements were performed at a given *L* shell is overplotted by the blue curve on the figure. Figure 9b presents the occurrence rate of dayside QP emissions as a function of *L* shell. Considering the large interval of *L* shells where the QP emissions occur (Figure 9), and variations of their occurrence rate as a function of longitude, we have examined if any of the parameters shown in Figures 3–6 depends on the spacecraft position. The results indicate that these parameters are not clearly dependent on the position.

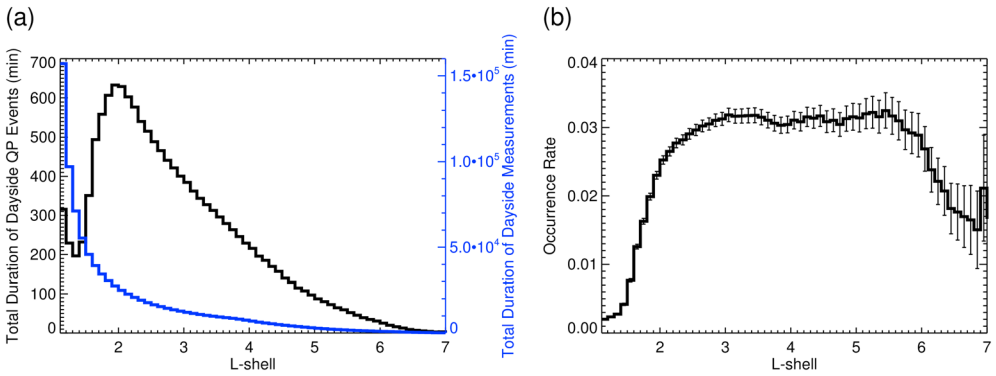

Figure 9. (a) Total duration of dayside QP events as a function of L shell shown by the black line. The blue curve (right axis) represents the total duration of DEMETER dayside measurements. (b) The occurrence rate of dayside QP events calculated from Figure 9a as a function of L shell. Error bars have been calculated from the binomial distribution, counting the number of median modulation periods.

4. Discussion

The database of QP events used in the analysis was prepared manually, by a visual inspection of all the electric field data measured by the DEMETER spacecraft. This necessarily involves some inaccuracies stemming from a subjectivity of a person visually inspecting the data. However, a possibility of a QP event being falsely identified is effectively minimalized by checking each relevant time interval twice—once during the identification itself and once during the process of three-point characterization of individual QP elements. Nevertheless, we cannot exclude a possibility that some of the QP events present in the DEMETER data set have been missed during the identification process and do not therefore contribute to the resulting statistics. However, taking into account the large numbers of analyzed events, a few events that we might have possibly missed seem unlikely to be able to affect significantly the obtained results. In order to further verify the robustness of the obtained results, we have performed exactly the same analysis not only with the whole DEMETER data set but also with selected data subsets. No significant differences between the obtained results have been found.

Figure 2 shows that QP emissions occur preferentially after periods of larger geomagnetic activity. Although this change of average values of geomagnetic indices is statistically significant, its absolute value is small compared to typical fluctuations of the indices. The observed increase of *Kp* index before QP emissions is less than 1, while the standard deviation of the distribution of *Kp* index values over the DEMETER mission is about 1.3. Similarly, the observed variation in the *AE* index is about 130 nT, while the standard deviation of the distribution of *AE* index values over the DEMETER mission is about 175 nT. This means that although the occurrence of QP emissions is on average linked to the geomagnetic activity, and in a given randomly chosen particular case the values of geomagnetic indices can vary rather differently.

The minimum frequency of QP elements (blue curve in Figure 3b) might be determined by the local multi-ion cutoff frequency. It can be clearly seen in Figure 1a, where the observed intensity of electromagnetic waves abruptly decreases at the frequencies below about 600 Hz. The presence of this cutoff will necessarily affect also the frequency bandwidth results depicted in Figure 4, and it possibly can, at least partially, explain why elements with larger central frequencies have larger bandwidths (Figure 4b). The frequency of this cutoff is related to the proton cyclotron frequency and ion composition at the satellite altitude [*Gurnett and Burns*, 1968; *Santolík et al*., 2006a]. Hence, it strongly varies with the spacecraft position. Our data, however, indicate that the minimum frequency of QP elements does not clearly depend on the geomagnetic latitude or longitude of the spacecraft. The minimum frequency of QP elements is therefore likely not determined by the local plasma parameters. It is rather probably connected to the generation mechanisms which would, in this case, produce the sharp peak at about 600 Hz seen in Figure 3b.

The distribution of modulation periods (Figure 5a), their relationship with the frequency drift of QP elements (Figure 6a), and the analysis of wave amplitudes (Figure 7), can give valuable experimental input for theoretical modeling of the conditions in the source region of QP emissions. However, a full understanding of these dependencies requires a significant additional data analysis effort and theoretical development, which is far beyond the scope of the present experimental paper.

Manninen et al. [2012] presented ground-based simultaneous observations of the periodically changing VLF emissions and geomagnetic pulsations. Authors concluded that VLF emissions accompanied by geomagnetic pulsations were not similar in their morphological properties to the known QP1 and QP2 types. However, the spectral form of observed emissions was explained well within the framework of theoretical predictions by *Bespalov* [1981] and *Bespalov and Koval'* [1982], and the QP emissions were classified as QP2 type. Simultaneous geomagnetic pulsations were considered as a consequence of the QP emissions generation process. The emissions analyzed by *Manninen et al*. [2012] had periods from 20 s to 60 s and a high frequency drift. Taking into account these results, we can associate the QP events from our data set with parameters similar to the event studied by *Manninen et al*. [2012] (majority of our cases) to the QP2 type.

The results from Figure 8 show that there are less QP events occurring at the longitudes of the Atlantic Ocean. *Němec et al*. [2009] have found similar effect when analyzing the occurrence of Magnetospheric line radiation (MLR) events. After comparing the longitudinal distribution of electron fluxes obtained by *Asikainen and Mursula* [2008] with the MLR distribution, they suggested that the decreased occurrence of MLR events might be due the lack of energetic electrons at this longitudinal range, as their significant amount is precipitated in the region of the South Atlantic anomaly. We believe that a similar explanation might be possibly used also for the decreased occurrence rate of emissions of the QP2 type, suggesting that their generation is related to energetic electrons [*Demekhov and Trakhtengerts*, 1994]. The decreased number of the QP2 emissions observed above the South Atlantic anomaly can result in a lower occurrence rate of the QP emissions in this region.

Figure 9 shows that QP emissions occur primarily at geomagnetic latitudes larger than about 30° ($L > \sim 2$), while the upper limit of the geomagnetic latitudes (L shells) of their occurrence could not be determined due to technical limitations of the DEMETER satellite, whose measurements are limited to geomagnetic latitudes lower than about 65° ($L < \sim 7$).

5. Conclusion

We presented results of a statistical analysis of QP emissions based on observations by the low-altitude DEMETER spacecraft. According to our knowledge, the analyzed data set represents the largest collection of satellite observations of QP emissions available to date (2264 events). The QP emissions were found to occur in about 5% of daytime half orbits with DEMETER measurements. The QP events were defined to have at least two elements anywhere along the spacecraft trajectory. Taking into account the average duration of the QP events (~15 min) and the average duration of half orbits (~40 min), QP emissions were found to occur in ~2% of observational time. On the other hand, QP events are basically absent during the night. This confirms that QP emissions are mostly dayside phenomena. QP emissions occur most often at frequencies from ~750 Hz to 2 kHz, but they may be observed at frequencies as low as ~500 Hz and as high as ~8 kHz. Modulation periods of QP events can vary from 10 to 100 s, with a typical value of about 20 s. The main results concerning the properties of the observed QP emissions can be summarized as follows: (1) QP events occur preferentially after periods of increased geomagnetic activity, at the times when it returns back to normal levels. (2) QP events with larger modulation periods have lower frequency drifts and smaller wave amplitudes. (3) Intense QP events have higher frequency drifts and larger values of the frequency bandwiths. (4) A typical change of the QP modulation period is usually on the order of about 20% during a single QP event. (5) QP emissions occur over a large interval of geomagnetic latitudes corresponding to $L \geq 2$, and their properties are not clearly dependent on the spacecraft position. (6) The occurrence rate of QP emissions is lower at the longitudes of the Atlantic Ocean which are known to be influenced by the geomagnetic field peculiarities in the South Atlantic anomaly.

Technical limitations of the DEMETER spacecraft do not allow us to make a clear conclusion about the source of QP emissions or to separate the observed QP events into the QP1 or QP2 types of emissions.

Acknowledgments

This investigation is based on observations performed by the DEMETER satellite launched by the Centre National d'Etudes Spatiales. The authors thank J.J. Berthelier, the PI of the ICE instrument, for the use of the data. This work was supported by the P209/11/2280 and P209/12/P658 grants of the Grant Agency of the Czech Republic and by grants LH 12231 and M100421206; the work of M.P. is supported by the Centre National d'Etudes Spatiales.

Michael Balikhin thanks the reviewers for their assistance in evaluating the paper.

References

Asikainen, T., and K. Mursula (2008), Energetic electron flux behavior at low L-shells and its relation to the South Atlantic anomaly, *J. Atmos. Sol. Terr. Phys.*, *70*, 5322–538.

Berthelier, J. J., et al. (2006), ICE, the electric field experiment on DEMETER, *Planet. Space Sci.*, *54*, 456–471.

Bespalov, P. A. (1981), Self-modulation of radiation of a plasma cyclotron maser, *JETP Lett.*, *33*(4), 182–185.

Bespalov, P. A. (1982), Self-excitation of periodic cyclotron instability regimes in a plasma magnetic trap, *Phys. Scr.*, 575–579, doi:10.1088/0031-8949/1982/T2B/044.

Bespalov, P. A., and L. N. Koval' (1982), Establishment of periodic regimes of cyclotron instability in plasma magnetic mirrors, *Fiz. Plazmy*, *8*(6), 1136–1144.
Bespalov, P. A., and V. Y. Trakhtengerts (1976), The dynamics of the cyclotron instability in a magnetic trap, *Fiz. Plazmy*, *2*(3), 397–406.
Carson, W. B., J. A. Koch, J. H. Pope, and R. M. Gallet (1965), Long period very low frequency emission pulsations, *J. Geophys. Res.*, *70*(17), 4293–4303, doi:10.1029/JZ070i017p04293.
Chen, L. (1974), Theory of ULF modulation of VLF emissions, *Geophys. Res. Lett.*, *1*(2), 73–75, doi:10.1029/GL001i002p00073.
Davidson, G. T. (1979), Self-modulated VLF wave-electron interactions in the magnetosphere: A cause of auroral pulsations, *J. Geophys. Res.*, *84*(A11), 6517–6523, doi:10.1029/JA084iA11p06517.
Demekhov, A. G., and V. Y. Trakhtengerts (1994), A mechanism of formation of pulsating aurorae, *J. Geophys. Res.*, *99*(4), 5831–5841, doi:10.1029/93JA01804.
Engebretson, M. J., J. L. Posch, A. J. Halford, G. A. Shelburne, A. J. Smith, M. Spasojević, U. S. Inan, and R. L. Arnoldy (2004), Latitudinal and seasonal variations of quasiperiodic and periodic VLF emissions in the outer magnetosphere, *J. Geophys. Res.*, *109*, A05216, doi:10.1029/2003JA010335.
Gurnett, D. A., and T. B. Burns (1968), The low-frequency cutoff of elf emissions, *J. Geophys. Res.*, *73*, 7437–7445, doi:10.1029/JA073i023p07437.
Hayosh, M., D. L. Pasmanik, A. G. Demekhov, O. Santolík, M. Parrot, and E. E. Titova (2013), Simultaneous observations of quasi-periodic ELF/VLF wave emissions and electron precipitation by DEMETER satellite: A case study, *J. Geophys. Res. Space Physics*, *118*, 1–11, doi:10.1002/jgra.50179.
Helliwell, R. A. (1965), *Whistlers and Related Ionospheric Phenomena*, Stanford Univ. Press, Stanford, Calif.
Ho, D. (1973), Interaction between whistlers and quasiperiodic VLF emissions, *J. Geophys. Res.*, *78*(31), 7347–7356, doi:10.1029/JA078i031p07347.
Kimura, I. (1974), Interrelation between VLF and ULF emissions, *Space Sci. Rev.*, *16*, 389–411.
Kitamura, T., J. A. Jacobs, T. Watanabe, and J. R. B. Flint (1969), An investigation of quasi-periodic VLF emissions, *J. Geophys. Res.*, *74*(24), 5652–5664, doi:10.1029/JA074i024p05652.
Manninen, J., T. Turunen, J. Kultima, and E. Titova (1994), Correlating optical emissions, quasi-periodic very low frequency emission and magnetic Pc3 pulsations, *Geomagn. Aeron.*, *34*, 42–47.
Manninen, J., N. G. Kleimenova, O. V. Kozyreva, P. A. Bespalov, and T. Raita (2012), Quasi-periodic very low frequency emissions, very low frequency chorus, and geomagnetic *Pc*4 pulsations (Event on April 3, 2011), *Geomagn. Aeron.*, *52*(1), 77–87.
Manninen, J., N. G. Kleimenova, O. V. Kozyreva, P. A. Bespalov, and A. E. Kozlovsky (2013), Non-typical ground-based quasi-periodic VLF emissions observed at $L \sim 5.3$ under quiet geomagnetic conditions at night, *J. Atmos. Sol. Terr. Phys.*, *99*, 123–128.
Manninen, J., A. G. Demekhov, E. E. Titova, A. E. Kozlovsky, and D. L. Pasmanik (2014), Quasiperiodic VLF emissions with short-period modulation and their relationship to whistlers: A case study, *J. Geophys. Res. Space Physics*, *119*, 3544–3557, doi:10.1002/2013JA019743.
Morrison, K. (1990), Quasiperiodic VLF emissions and concurrent magnetic pulsations seen at $L = 4$, *Planet. Space Sci.*, *38*(12), 1555–1565.
Morrison, K., M. J. Engebretson, J. R. Beck, J. E. Johnson, R. L. Arnoldy, J. L. J. Cahill, D. L. Carpenter, and M. Gallani (1994), A study of quasi-periodic ELF-VLF emissions at three antarctic stations: Evidence for off-equatorial generation?, *Ann. Geophys.*, *12*, 139–146, doi:10.1007/s00585-994-0139-8.
Němec, F., M. Parrot, O. Santolík, C. J. Rodger, M. J. Rycroft, M. Hayosh, D. Shklyar, and A. Demekhov (2009), Survey of magnetospheric line radiation events observed by the DEMETER spacecraft, *J. Geophys. Res.*, *114*, A05203, doi:10.1029/2008JA014016.
Němec, F., O. Santolík, M. Parrot, J. S. Pickett, M. Hayosh, and N. Cornilleau-Wehrlin (2013a), Conjugate observations of quasiperiodic emissions by Cluster and DEMETER spacecraft, *J. Geophys. Res. Space Physics*, *118*, 198–208, doi:10.1029/2012JA018380.
Němec, F., O. Santolík, J. S. Pickett, M. Parrot, and N. Cornilleau-Wehrlin (2013b), Quasi-periodic emissions observed by the Cluster spacecraft and their association with ULF magnetic pulsations, *J. Geophys. Res. Space Physics*, *118*, 4210–4220, doi:10.1002/jgra.50406.
Parrot, M. (Ed.) (2006), First results of the DEMETER micro-satellite, *Planet. Space Sci.*, *54*, 411–558.
Parrot, M., et al. (2006), The magnetic field experiment IMSC and its data processing onboard DEMETER: Scientific objectives, description and first results, *Planet. Space Sci.*, *54*, 441–455.
Pasmanik, D. L., A. G. Demekhov, V. Y. Trakhtengerts, E. E. Titova, O. Santolík, F. Jiricek, J. Smilauer, K. Kudela, and M. Parrot (2004), Quasi-periodic ELF/VLF wave emissions in the Earth's magnetosphere: Comparison of satellite observations and modeling, *Ann. Geophys.*, *22*, 4351–4361.
Santolík, O., and M. Parrot (1999), Case studies on wave propagation and polarization of ELF emissions observed by Freja around the local proton gyro-frequency, *J. Geophys. Res.*, *104*(A2), 2459–2475, doi:10.1029/1998JA900045.
Santolík, O., and M. Parrot (2000), Application of wave distribution function methods to an ELF hiss event at high latitudes, *J. Geophys. Res.*, *105*, 18,885–18,894, doi:10.1029/2000JA900029.
Santolík, O., F. Němec, M. Parrot, D. Lagoutte, L. Madrias, and J. J. Berthelier (2006a), Analysis methods for multi-component wave measurements on board the DEMETER spacecraft, *Planet. Space Sci.*, *54*, 512–527.
Santolík, O., J. Chum, M. Parrot, D. A. Gurnett, J. S. Pickett, and N. Cornilleau-Wehrlin (2006b), Propagation of whistler mode chorus to low altitudes: Spacecraft observations of structured ELF hiss, *J. Geophys. Res.*, *111*, A10208, doi:10.1029/2005JA011462.
Sato, N., and H. Fukunishi (1981), Interaction between ELF-VLF emissions and magnetic pulsations: Classification of quasiperiodic ELFVLF emissions based on frequencytime spectra, *J. Geophys. Res.*, *86*(A1), 19–29, doi:10.1029/JA086iA01p00019.
Sato, N., and S. Kokubun (1980), Interaction between ELF-VLF emissions and magnetic pulsations: Quasiperiodic ELFVLF emissions associated with Pc 3-4 magnetic pulsations and their geomagnetic conjugacy, *J. Geophys. Res.*, *85*(A1), 101–113, doi:10.1029/JA085iA01p00101.
Sato, N., and S. Kokubun (1981), Interaction between ELF-VLF emissions and magnetic pulsations: Regular period ELFVLF pulsations and their geomagnetic conjugacy, *J. Geophys. Res.*, *86*(A1), 9–18, doi:10.1029/JA086iA01p00009.
Sato, N., and T. Matsudo (1986), Origin of magnetic pulsations associated with regular period VLF pulsations (Type 2 QP) observed on the ground at Syowa station, *J. Geophys. Res.*, *91*(A10), 11,179–11,185, doi:10.1029/JA091iA10p11179.
Sato, N., K. Hayashi, S. Kokubun, T. Oguti, and H. Fukunishi (1974), Relationships between quasiperiodic VLF emission and geomagnetic pulsation, *J. Atmos. Sol. Terr. Phys.*, *36*, 1515–1526.
Sazhin, S. S. (1987), An analytical model of quasiperiodic ELFVLF emissions, *Planet. Space Sci.*, *35*(10), 1267–1274.
Sazhin, S. S., and M. Hayakawa (1994), Periodic and quasiperiodic VLF emissions, *J. Atmos. Sol. Terr. Phys.*, *56*(6), 735–753.
Smith, A. J., D. L. Carpenter, Y. Corcuff, J. P. S. Rash, and E. A. Bering (1991), The longitudinal dependence of whistler and chorus characteristics observed on the ground near $L = 4$, *J. Geophys. Res.*, *96*(A1), 275–284, doi:10.1029/90JA01077.
Smith, A. J., M. J. Engebretson, E. M. Klatt, U. S. Inan, R. L. Arnoldy, and H. Fukunishi (1998), Periodic and quasiperiodic ELF/VLF emissions observed by an array of Antarctic stations, *J. Geophys. Res.*, *103*(A10), 23, 611–23, 622, doi:10.1029/98JA01955.
Tixier, M., and N. Cornilleau-Wehrlin (1986), How are the VLF quasiperiodic emissions controlled by harmonics of field line oscillations? The results of a comparison between ground and GEOS satellites measurements, *J. Geophys. Res.*, *91*(A6), 6899–6919, doi:10.1029/JA091iA06p06899.
Watt, C. E. J., A. W. Degeling, R. Rankin, K. R. Murphy, I. J. Rae, and H. J. Singer (2011), Ultra low frequency modulation of whistler mode wave growth, *J. Geophys. Res.*, *116*, A10209, doi:10.1029/2011JA016730.